The Fibrillar Substructure of Keratin Filaments Unraveled

UELI AEBI, WALTER E. FOWLER, PAMELA REW, and TUNG-TIEN SUN*
Department of Cell Biology and Anatomy, and Departments of Dermatology and Ophthalmology, The Johns Hopkins University School of Medicine, Baltimore, Maryland 21205. Dr. Sun's present address is the Departments of Dermatology and Pharmacology, New York University School of Medicine, New York 10016.

ABSTRACT We show that intermediate-sized filaments reconstituted from human epidermal keratins appear unraveled in the presence of phosphate ions. In such unraveling filaments, up to four "4.5-nm protofibrils" can be distinguished, which are helically twisted around each other in a right-handed sense. Lowering the pH of phosphate-containing preparations causes the unraveling filaments to further dissociate into "2-nm protofilaments." In addition, we find that reconstitution of keratin extracts in the presence of small amounts of trypsin yields paracrystalline arrays of 4.5-nm protofibrils with a prominent 5.4-nm axial repeat. Limited proteolysis of intact filaments immobilized on an electron microscope grid also unveils the presence of 4.5-nm protofibrils within the filament with the same 5.4-nm axial repeat. These results, together with other published data, are consistent with a 10-nm filament model based on three distinct levels of helical organization: (*a*) the 2-nm protofilament, consisting of multichain extended alpha-helical segments coiled around each other; (*b*) the 4.5-nm protofibril, being a multi-stranded helix of protofilaments; and (*c*) the 10-nm filament, being a four-stranded helix of protofibrils.

Intermediate-sized filaments have been found in virtually all vertebrate cell types and, while they can be grouped into five different classes according to their biochemical and immunological properties, they all have a similar morphology (1–4). Whether native or reconstituted, they appear in the electron microscope as long, unbranched structures having diameters ranging from 7 to 11 nm—hence the name "10-nm filaments." The polypeptides making up these filaments have been shown by various techniques to be folded largely into extended alpha-helical segments and to associate laterally to form coiled-coils parallel to the filament axis (5–13). Based on such data and on models formulated earlier for the alpha-keratin microfibril (6) and epidermal prekeratin (5, 14), Steinert proposed the "three-chain structural unit" or "2-nm protofilament" to be the building block for bovine epidermal keratin filaments in particular (7) and intermediate-sized filaments in general (8). However, results from recent crosslinking studies (12) suggest that the protofilament unit is built as a dimer of interchain double-stranded coiled-coils. While protofilaments with apparent diameters of 2–3 nm have been visualized within most types of native and reassembled intermediate-sized filaments under appropriate conditions (9, 15–19), relatively little is known concerning the number and helical organization of the 2-nm protofilaments within the 10-nm filament (19, 20). In addition, although 3–5 nm wide "strands" (17) or "subfilaments" (18) have been observed in disassembling filaments, their quantitative relationship with either the 10-nm filament or the 2-nm protofilament has remained unclear.

Here we present results obtained by electron microscopy of 10-nm filaments reconstituted from human epidermal cell keratins that have been (*a*) negatively stained with different heavy metal salts, (*b*) treated with phosphate and other charged molecules, or (*c*) subjected to limited proteolysis. Our findings demonstrate that "4.5-nm protofibrils" are the intermediate building blocks for the 10-nm filament. From unraveling filaments, we attempt to derive the number and helical parameters of these protofibrils within the filament and to demonstrate that the protofibril itself consists of "2-nm protofilaments." In addition, we document a 5.4nm axial repeat along the length of the protofibril. Based on these data, a consistent model in terms of three distinct levels of helical organization—the 2-nm protofilament, the 4.5-nm protofibril, and the 10-nm filament—is formulated and subsequently

THE JOURNAL OF CELL BIOLOGY · VOLUME 97 OCTOBER 1983 1131-1143

evaluated in view of pre-existing data and models relating to the structure of keratin and other intermediate-sized filaments.

MATERIALS AND METHODS

Reconstitution of Keratin Filaments: Human epidermal cell keratins were extracted from either cultured epidermal keratinocytes ("HE")[1] or in vivo callus ("callus") with 8 M urea/25 mM dithiothreitol (DTT) according to a protocol described earlier (21). Filaments were reconstituted by diluting the urea/DTT keratin fraction to 1 mg/ml with 10 mM Tris-HCl, pH 7.5, 8 M urea, and 50 mM DTT, incubating for 3 h at 37°C, taking a 10-min 100,000 *g* supernatant and dialyzing it for 15 h at 4°C against "filament buffer" consisting of 5 mM Tris, 1 mM DTT, 15 mM KCl, pH 7.5. Under all conditions tried in this study, reconstituted HE and callus keratin filaments were indistinguishable from each other when visualized in the electron microscope.

Preparation of Negatively Stained Keratin Filaments: Reconstituted HE or callus keratin filaments (1 mg/ml) were diluted to 0.25 mg/ml with filament buffer before 3-μl aliquots were adsorbed for 60 s to a hydrophilic (i.e., by glow discharge) carbon support film, washed for 30 s with H_2O, and stained for 30 s with 0.75% uranyl formate, pH 4.25; excess stain was drained off before the grid was allowed to air-dry. The same protocol was also followed using gold thio-glucose (22) as the negative stain. Alternatively, reconstituted HE or callus keratin filaments (0.5 mg/ml) were diluted 1:1 with 2% sodium phosphotungstate (NaPT), pH 7.0, left for up to 60 s at room temperature, adsorbed for 60 s to a hydrophilic carbon support film, and allowed to air-dry (without washing) after excess liquid was drained off.

Treatment of Keratin Filaments with Phosphate Buffer: HE or callus keratin extracts (1 mg/ml) were reconstituted by dialysis against filament buffer containing 5–25 mM Na- or K-phosphate instead of Tris (see Reconstitution of Keratin Filaments above). Alternatively, HE or callus keratin filaments (1 mg/ml) reconstituted in Tris-filament buffer (see Reconstitution of Keratin Filaments above) were diluted to 0.125 mg/ml with 1–25 mM Na-phosphate, pH 6.0–7.5 (see Results), and left for 1 min to 1 h at 4°C. 3-μl aliquots were then adsorbed for 60 s to hydrophilic carbon support films, washed for 30 s with H_2O, and stained for 30 s with 0.75% uranyl formate, pH 4.25, before excess liquid was drained off and the grids were allowed to air-dry. Treatment with other charged molecules followed the same protocol.

Preparation of Metal Shadowed Specimens: Glycerol-sprayed/vacuum-dried filaments in either Tris or phosphate buffer were prepared on mica as described (23–25). For freeze-drying, 3-μl aliquots of freshly reconstituted (see Reconstitution of Keratin Filaments above) or phosphate-treated (see above) filaments at the same dilution used for negative staining (see previous two sections above) were adsorbed to a glow-discharged carbon support film, washed for 10 s with H_2O, blotted with filter paper, and immediately plunged into liquid nitrogen. Frozen samples were freeze-dried as described (25–27). Specimens on mica or carbon substrates were unidirectionally or rotary shadowed with platinum/carbon or tantalum/tungsten at an elevation angle of ~15° in a Balzers BAF 400 freeze-etching unit. Replicas on mica were floated off onto a distilled water surface and picked up on uncoated 400-mesh/inch copper grids.

Limited Proteolysis: HE keratin urea/DTT extracts (see above, Reconstitution of Keratin Filaments) were diluted to 1 mg/ml with 10 mM Tris, 8 M urea, 50 mM DTT, pH 7.5, incubated for 3 h at 37°C and centrifuged for 10 min at 100,000 *g*. Trypsin (bovine pancreas, Type XI; Sigma Chemical Co., St. Louis, MO) was added to the resulting supernatant (1 to 5 μg/ml final concentration) and the mixture was dialyzed for 15 h at 4°C against filament buffer (see above, Reconstitution of Keratin Filaments). The resulting samples were prepared for negative-stain electron microscopy as described above in Preparation of Negatively Stained Keratin Filaments. Alternatively, reconstituted HE keratin filaments (1 mg/ml) were diluted to 0.25 mg/ml with filament buffer, and 3-μl aliquots were adsorbed for 60 s to hydrophilic carbon support films. Excess liquid was blotted off with filter paper and immediately replaced with a 3-μl aliquot of filament buffer containing 1–10 μg/ml of trypsin (bovine pancreas, Type XI; Sigma Chemical Co.). The reaction was stopped after 1–10 min by washing for 30 s with H_2O followed by negative staining with 0.75% uranyl formate as described above in Preparation of Negatively Stained Keratin Filaments.

Electron Microscopy: Negatively stained or metal-shadowed specimens were examined in a Zeiss EM10C electron microscope that was operated at an accelerating voltage of 80 kV. Electron micrographs were recorded at either 25,000 or 50,000 times nominal magnification on Kodak SO-163 electron image film and developed for 4 min at 20°C in Kodak D-19 diluted 1:2 with H_2O. Magnification calibration was performed according to Wrigley (28) using negatively stained catalase crystals. Micrographs of metal-shadowed specimens (see Fig. 3) were printed with reverse contrast (i.e., shadows appear dark).

[1] *Abbreviations used in this paper:* DTT, dithiothreitol; HE, cultured epidermal keratinocytes; NaPT, sodium phosphotungstate.

RESULTS

(a) Effect of Different Negative Stains on the Appearance of Keratin Filaments

Intermediate-sized filaments freshly reconstituted from human epidermal cell keratins (Fig. 1 *a*) that have been negatively stained with uranyl formate or uranyl acetate have an apparent average width (as measured from their stain exclusion profile) of ~9 nm in diameter (Table I) and display little or no obvious fibrillar substructure (Fig. 1 *b*). Filaments that have been negatively stained with gold thio-glucose (22) give similar results, although the contrast of the filaments is markedly reduced. This diameter probably represents a lower limit, since the filaments are partially embedded in negative stain, making the filament edges somewhat ambiguous. When NaPT is used as the negative stain, the average filament width increases to ~11.5 nm (Table I), and a distinct fibrillar substructure becomes apparent along the length of the unraveling filaments (Fig. 1 *c*). Up to four "protofibrils" can be distinguished (see arrowheads in Fig. 1 *c*) whose widths, as delineated by their stain exclusion profiles, vary from 2.2 to 3.7 nm with an average of 3 nm (Table I). For the reasons given above, these figures are most likely underestimates of the actual protofibril diameter. In contrast, the center-to-center distance between these protofibrils is relatively constant and measures 4.5 nm on average (Table I). However, it is possible that the unraveling protofibrils are no longer in tight contact with each other along their whole length and the measured inter-protofibril distance may therefore represent an overestimate of the protofibril diameter. The "true" protofibril diameter therefore probably lies somewhere between 3 and 4.5 nm. With regard to the number of protofibrils per filament, the data are most compatible with four, since in projection a four-stranded helix will display either two or three strands with all four strands being apparent only after substantial untwisting and/or spread-flattening of the filament (see also Figs. 2, *a* and *b*, and 3 *d*).

(b) Effect of Phosphate and Other Ions on Keratin Filaments

With the aim of further unraveling the fibrillar substructure of keratin filaments, we investigated the effects of various buffers and ions on the appearance of reconstituted filaments in the electron microscope. Filaments reconstituted in Na- or K-phosphate, pH 7.5, instead of Tris buffer, appeared "unraveled" to various degrees, as is illustrated with representative examples in Fig. 2 *a*: long, unraveled filament stretches are interspersed with shorter, more or less compact filament stretches. To determine whether these filaments represented a misassembled species, we took filaments that were freshly reconstituted in Tris buffer and diluted them with phosphate buffer 1 min to 1 h before specimen preparation (Fig. 2 *b*). Filaments treated in this way appeared indistinguishable from the filaments reconstituted in phosphate buffer (Fig. 2 *a*). For both types of phosphate-treated preparations the extent of unraveling of the filaments clearly increased with increasing phosphate concentration. As with NaPT staining (Fig. 1 *c*), up

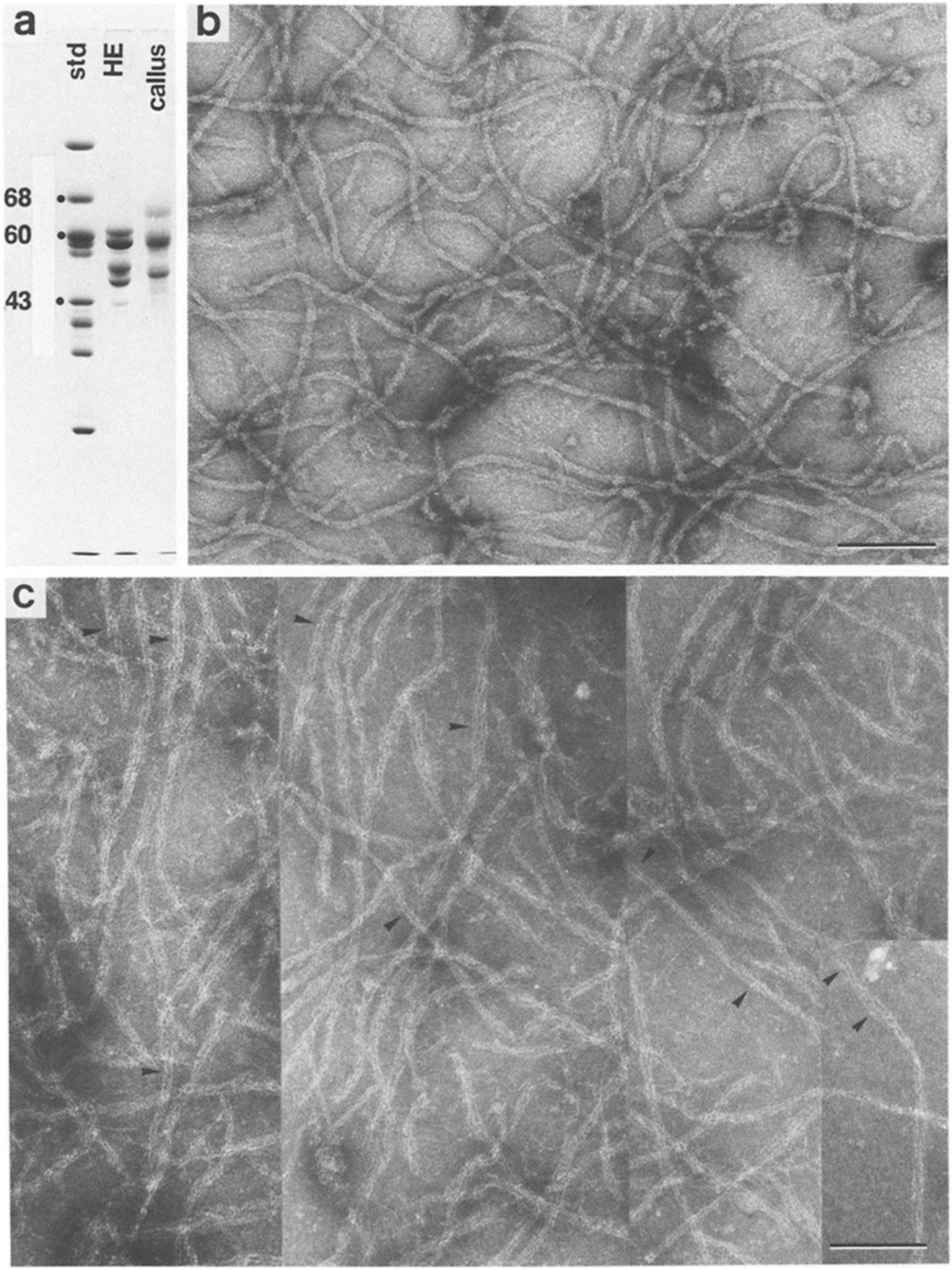

FIGURE 1 Polypeptide composition and electron micrographs of intermediate-sized filaments reconstituted from human epidermal cell keratins. (*a*) 10% polyacrylamide SDS gel electrophoresis of keratin extracts from cultured epidermal keratinocytes (*HE*) and in vivo callus (*callus*) as they were used for filament reconstitutions; gel standards (*std*) include actin (43,000 mol wt), catalase (60,000 mol wt) and bovine serum albumin (68,000 mol wt). (*b*) Reconstituted HE filaments negatively stained with 0.75% uranyl formate, pH 4.25. Note the absence of apparent fibrillar substructure. (*c*) Reconstituted HE filaments negatively stained with 2% sodium phosphotungstate, pH 7.0. Arrowheads point to filament stretches where protofibrils (see text) can be distinguished. Bars, 100 nm. (*b* and *c*) × 180,000.

TABLE I

Parameters Defining the Fibrillar Architecture of Keratin Filaments

Preparation	Filament width(nm)	Protofibril width(nm)/ [1]Protofilament width(nm)	Protofibril-to-protofibril distance(nm)	Cross over repeats(nm)/ [2]Axial repeat along protofibril(nm)
HE in Tris; negatively stained with 0.75% uranyl formate, pH 4.25	9.2 ± 0.5/7.9/10.1(84)	—	—	—
Callus in Tris; negatively stained with 0.75% uranyl formate, pH 4.25	9.0 ± 0.4/8.2/9.8(103)	—	—	—
HE in Tris; negatively stained with 2% sodium phosphotungstate, pH 7.0	11.5 ± 1.2/8.0/14.9 (186)	3.0 ± 0.4/2.2/3.7(190)	4.5 ± 0.2/4.0/5.3(5)	—
Callus in 10 mM Na-phosphate, pH 7.5; negatively stained with 0.75% uranyl formate, pH 4.25	—	3.8 ± 0.4/2.9/4.4(81)	—	23.7 ± 2.8/17.3/29.1(43) 45.8 ± 4.5/38.1/54.4(169) 92.6 ± 6.5/79.8/108.8(165)
Callus in Tris; glycerol-dried/unidirectionally shadowed with Pt/carbon	—	—	—	22.9 ± 2.4/17.1/28.3(164)
Callus in 10 mM Na-phosphate; pH 7.5; freeze-dried unidirectionally shadowed with Pt/carbon	—	—	—	46.7 ± 3.6/37.6/56.5(103) 92.0 ± 6.8/81.1/111.7(318)
Callus in 10 mM Na-phosphate; pH 7.5 freeze-dried/rotary shadowed with Pt/carbon	12.6 ± 1.0/10.2/15.3(145)	—	—	46.1 ± 3.8/39.2/54.5(88) 92.1 ± 6.2/79.9/110.1(209)
Callus in 10 mM Na-phosphate, pH 6.25; negatively stained with 0.75% uranyl formate, pH 4.25	—	[1]2.2 ± 0.3/1.6/2.9(76)	—	—
He extract reconstituted in Tris in the presence of trypsin; negatively stained with 0.75% uranyl formate, pH 4.25	—	3.4 ± 0.4/2.6/3.9(61)	4.4 ± 0.1/4.2/4.7(38)	[2]5.4 ± 0.08/5.1/5.6(42)
HE in Tris; proteolysed with trypsin on the grid; 0.75% uranyl formate, pH 4.25	11.4 ± 1.8/8.3/13.3(31)	3.5 ± 0.3/2.5/3.7(77)	4.5 ± 0.1/4.2/4.8(55)	[2]5.4 ± 0.06/5.2/5.5(59)

HE/Callus: intermediate-sized filaments reconstituted from human epidermal keratins extracted from either cultured epidermal keratinocytes (*HE*) or in vivo callus (Callus) (see Fig. 1); all measurements include: mean ± rms/min/max(*n*), where *n* is the number of measurements, "*mean*" is the mean value from a set of *n* measurements, "*rms*" is the root mean square deviation from the mean, "*min*" and "*max*" are the minimal and maximal values included in the set of measurements.

to four "protofibrils" can be distinguished within such unraveled filament stretches. In some places, the protofibrils themselves seem to unravel, making determination of their exact number more difficult. The apparent width of these protofibrils, as measured from their stain exclusion profiles, is 3.8 nm on average (Table I). The protofibrils "wave" back and forth and cross each other, giving the impression of being helically twisted around each other, most often in a right-handed sense. Cross overs occur at more or less regular intervals along the filaments. While individual measurements

of the crossover repeats can vary appreciably (Table I), the average values, 45.8 and 92.6 nm, are well conserved between independent sets of measurements. These variations are most likely due to local under- or overwinding of the unraveled multi-stranded filaments or to spread-flattening during specimen preparation. Occasionally, shorter crossover repeats can be distinguished that average ~23.7 nm (Table I).

We also tried reconstitution of keratin extracts in—or dilution of reconstituted filaments with—Na- or K-phosphate at different pHs. Most interestingly, pH 6.0–6.5 resulted in the appearance of a significant number of filaments that unraveled into "protofilaments" rather than protofibrils, as judged by their decreased apparent width and increased number (Fig. 2*c*). These protofilaments yielded a stain exclusion, the profile measuring 2.2 nm in width on average (see Table I). While it was difficult to unambiguously count the number of protofilaments per 10-nm filament (e.g., Fig. 2*c*), in some cases at least six could be distinguished. In most cases, either the filaments were not sufficiently unraveled to enable us to distinguish all the protofilaments or the filaments were completely unraveled and had apparently lost some protofilaments. Lowering the pH below 6.0 resulted in increasingly larger fibrillar aggregates, which appeared to be made of laterally aggregated protofilaments or protofibrils.

Filaments (1 mg/ml) diluted to 0.125 mg/ml with 5 mM Tris buffer, pH 7.5, looked indistinguishable from undiluted filaments (e.g., as in Fig. 1*b*). In contrast, filaments (1 mg/ml) diluted (to 0.125 mg/ml) with just H_2O started to unravel; their average apparent diameter increased to about 13 nm, but the extent of unraveling was significantly less than in the presence of phosphate. To determine the specificity of phosphate in unraveling reconstituted keratin filaments, we tested other negatively charged molecules such as glutamic and aspartic acid, and polyglutamic and polyaspartic acid. While all of these anions had a significant swelling and unraveling effect on intact filaments, the unraveling patterns looked quite distinct from those induced by either NaPT (Fig. 1*c*) or phosphate buffer (Fig. 2) when comparable concentrations of negative charges were used.

We also studied the effects of a variety of polycations (i.e., Mg^{++}, Ca^{++}, Mn^{++}, Co^{++}, Zn^{++}, Gd^{+++}, and polylysine) on the appearance of reconstituted filaments (see also reference 29). While every cation tested caused aggregation of the filaments when added in appropriate amounts, Ca^{++} and polylysine gave the most interesting results. Ca^{++} above ~5 mM caused the filaments to associate laterally into "folded ribbons" and other higher order aggregates, whereas polylysine (degree of polymerization 15–20) above ~0.01 mM resulted in compact and highly aligned bundles of filaments or protofibrils (P. Rew, W. E. Fowler and U. Aebi, manuscript in preparation). These bundles looked strikingly similar to the "macrofibrils" formed in the presence of filaggrin, a class of cationic proteins isolated from the stratum corneum of mammalian epidermis (30, 31).

In preliminary experiments, we have found that purified neurofilaments (a kind gift of Dr. Marschall Runge, Johns Hopkins University School of Medicine) appear also unraveled in the presence of 1–15 mM phosphate. We conclude that phosphate ions cause at least two types of 10-nm filament to swell or unravel to varying degrees. Although the mechanism underlying this unraveling process is not yet clear, this finding has allowed us to directly visualize the protofibrillar structure of keratin filaments.

(c) Appearance of Keratin Filaments After Metal Shadowing

We employed glycerol spraying/vacuum drying and adsorption/freeze-drying followed by high resolution unidirectional and rotary metal shadowing (25) to visualize the fibrillar substructure of reconstituted keratin filaments in the presence and absence of phosphate. Fig. 3*a* is a representative example of keratin filaments that were mixed with glycerol, sprayed on mica, dried in a vacuum evaporator, and unidirectionally shadowed with platinum/carbon (23, 24). As found previously (32, 33), such filaments do not display any fibrillar substructure but instead exhibit a "nodular" appearance with an average 23-nm axial repeat (Table I). This nodular appearance can also be visualized in glycerol-treated keratin filaments after negative staining (25) and thus appears to be an effect of "glycerol decoration" (34). Moreover, the fibrillar substructure of the keratin filaments appears to be stabilized by glycerol: i.e., unraveling, phosphate-treated filaments (e.g., Fig. 2, *a* and *b*) appear mostly intact (i.e., not unraveled) when prepared in the presence of 30% glycerol (25). Filaments in such preparations often display the 23-nm axial repeat seen in Fig. 3*a*, but show no fibrillar substructure. Although glycerol-sprayed/vacuum-dried filaments sometimes show an apparent handedness (33), we have found right- and left-handed filament stretches with about equal frequencies and sometimes along the length of the same filament. This apparently confusing result is discussed below in view of our filament model (see Discussion).

Filaments in phosphate buffer (see previous section) were also prepared by adsorption/freeze-drying (25–27) followed by rotary (Fig. 3*b*) or unidirectional (Fig. 3, *c* and *d*) shadowing. Much like after negative staining (Fig. 2, *a* and *b*), the filaments in these preparations frequently unravel into two to four distinguishable protofibrils that cross each other at more or less regular intervals, 47 nm or 92 nm on average (Table I). Note that some of the filaments in Fig. 3*d* (arrows) splay out into four protofibrils. The protofibrils are twisted around each other in a right-handed sense. This demonstration of the handedness is consistent with that seen in negatively stained preparations of phosphate-treated filaments (see previous section) and with results reported previously for quick-frozen and freeze-dried callus keratin filaments (34) and partially unraveled neurofilaments (17).

The average width for freeze-dried/rotary-shadowed filaments given in Table I, i.e. ~12.6 nm, has not been corrected for metal thickness and therefore is probably an overestimate. Experience (25, 34) suggests that the corrected value should be between 9 and 10 nm, which is consistent with our measurements of negatively stained filaments (Table I) and inconsistent with a value of 15 nm as recently proposed by Steven et al. (19, 20).

(d) Limited Proteolysis of Keratin Extracts and Immobilized Keratin Filaments

To gain complementary information about the fibrillar substructure of keratin filaments, we explored the effects of limited proteolysis on the ability of soluble keratin extracts to form filaments and on the structure of filaments that had been reconstituted prior to proteolysis. Dialysis of a mixture of HE keratin extract (1 mg/ml) with 1–5 μg/ml trypsin against Tris-filament buffer resulted in limited proteolysis.

The four major bands between 45 and 60 kdaltons seen by SDS gel electrophoresis of the fresh extract were converted to a set of distinct bands of lower molecular weight (Fig. 4, *a*): i.e., two bands between 30 and 40 kdaltons, at least three bands between 20 and 30 kdaltons and several bands between 10 and 20 kdaltons. Negatively stained preparations of such samples revealed virtually no intact 10-nm filaments. Much of the material retained on the electron microscope grid appeared in the form of filament debris and other random aggregates of variable size. However, a significant fraction of the proteolysed material was found in the form of bundles or paracrystalline arrays of laterally associated protofibrils (Fig. 4*b*). In places these bundles or paracrystals were aggregated further into large, three-dimensional structures. The apparent diameter of the constituent protofibrils, as measured by their stain exclusion profile, was 3.4 nm on average and the center-to-center spacing of adjacent protofibrils averaged 4.4 nm (Table I). In addition, these protofibrils exhibited a distinct 5.4 nm axial repeat that is not seen along the protofibrils of NaPT-stained (Fig. 1*c*) or phosphate-treated unproteolyzed filaments (Fig. 2, *a* and *b*). Since we have not yet been able to separate the aggregates made of 4.5-nm protofibrils from the remainder of the proteolyzed material, we are unable to unambiguously correlate these distinctive structures with one or more of the specific polypeptides known to be present in these preparations (Fig. 4*a*). However, we did find a correlation between the amount of protein in the two bands between 30 and 40 kdaltons and the number of bundles or paracrystals found in such proteolyzed samples. Filamentous bundles with a transverse striation having a similar periodicity have been observed previously in samples reconstituted from keratin extracts of psoriatic epidermis (35).

Alternatively, we incubated freshly reconstituted filaments, which were immobilized on carbon support films (i.e., EM grids), with various concentrations of trypsin (e.g., 1–10 μg/ml) for 1–10 min. Proteolysis was terminated by washing the grids with several drops of H_2O before staining them with uranyl formate. The digested material consisted of filament debris, as well as apparently intact filaments. In addition, we found a significant number of filament stretches that displayed the same distinctive fibrillar substructure (Fig. 5*a*) that was seen in bundles or paracrystals that formed upon reconstitution of keratin extracts in the presence of low levels of trypsin (Fig. 4*b*). Within these digested filament stretches, two to four protofibrils could be distinguished (see arrowheads in Fig. 5*a*); these protofibrils had an average stain exclusion width profile of 3.5 nm and a center-to-center spacing of 4.5 nm (Table I). Again a pronounced 5.4-nm axial repeat was apparent along these protofibrils. This repeat yields a meridional reflection at $(5.4\ \text{nm})^{-1}$ in optical diffraction patterns (Fig. 5*b*) recorded from such proteolyzed filament stretches (outlined by two arrows in Fig. 5*a*). In addition, these diffraction patterns display a near-equatorial layer line (indicated by arrowheads in Fig. 5*b*) related to a 16.2-nm pitch helix. The horizontal sampling of this layer line (i.e., the spacing of the intensity peak from the meridian) corresponds to a width that is roughly twice the inter-protofibril distance (i.e., 2 × 4.5 nm). Since adjacent protofibrils appear to be in register with respect to the 5.4-nm axial repeat, this sampling may indicate that adjacent protofibrils within the filament associate with alternating polarities (36, 37).

DISCUSSION

Despite recent advances in the biochemical characterization of intermediate filaments (7, 8, 10–13), relatively little is known about their fibrillar substructure and organization. Electron microscopic studies of the time course of assembly of different types of intermediate filaments have demonstrated the lateral and longitudinal aggregation of filamentous subparticles (17, 38–40). Likewise, examination of partially disassembled intermediate filaments has invariably revealed "strands" or "subfilaments" of various sizes (9, 15–19). However, conditions for the controlled dissection of any type of intermediate filament into distinct fibrillar substructures have yet to be established. In the present study, we have shown that keratin filaments unravel into distinct 4.5-nm protofibrils following treatment with phosphate ions at pH 7.5. These protofibrils can be visualized under a variety of conditions and therefore do not appear to represent a specimen preparation artifact (e.g., artificial aggregation of protofilaments). In addition, we have found that phosphate treatment at pH 6.0–6.5 causes keratin filaments to further unravel into 2-nm protofilaments.

The existence of a distinct "intermediate level of organization" between the 2-nm protofilament and the 10-nm filament—i.e. the 4.5-nm protofibril—within the reconstituted human epidermal keratin filaments used in this study has prompted us to formulate a tentative model involving three levels of fibrillar organization. These three levels are illustrated schematically as cross-sections in Fig. 6*a*: (I) the 2-nm protonfilament (whose effective diameter is more like 2.5–3.0 nm; see below); (II) the 4.5-nm protofibril; (III) the 10-nm filament. It has been suggested, based on data from x-ray diffraction (6, 9, 41–44), optical rotary dispersion and circular dichroism, (5, 7, 8, 10) and from primary sequence analysis (10–13, 45–49), that the 2-nm protofilament is made of either double- (6, 10, 12, 48–50) or triple- (5–8, 13) stranded coiled-coil alpha-helical segments that are oriented roughly parallel to the filament axis. Moreover, the results of chemical cross-linking experiments performed on wool alpha-keratin (51) and on a 40-kdalton fragment of desmin, which consists of

FIGURE 2 Unraveling effect of phosphate buffer on the appearance of keratin filaments. For electron microscopy samples were negatively stained with 0.75% uranyl formate, pH 4.25. (*a*) Filaments were reconstituted from callus extract in 15 mM Na-phosphate buffer, pH 7.5 (instead of 5 mM Tris), and diluted eightfold with the same buffer immediately before specimen preparation. (*b*) Callus keratin filaments which were reconstituted in Tris-filament buffer were diluted eightfold with 10 mM Na-phosphate, pH 7.5, 10 min prior to preparation for electron microscopy. The filaments in *a* and *b* appear to unravel into two to four 4.5-nm protofibrils (see text). (*c*) Callus keratin filaments which were reconstituted in Tris-filament buffer were diluted eightfold with 10 mM Na-phospbate, pH 6.25, 10 min prior to preparation for electron microscopy. At this pH the filaments appear to unravel into 2-nm protofilaments (see text) rather than into 4.5-nm protofibrils. While the number of 2-nm protofilaments is clearly more than four, it is difficult to count their exact number—often six to eight of them can be distinguished per filament. Bars, 100 nm. (*a–c*) × 145,000.

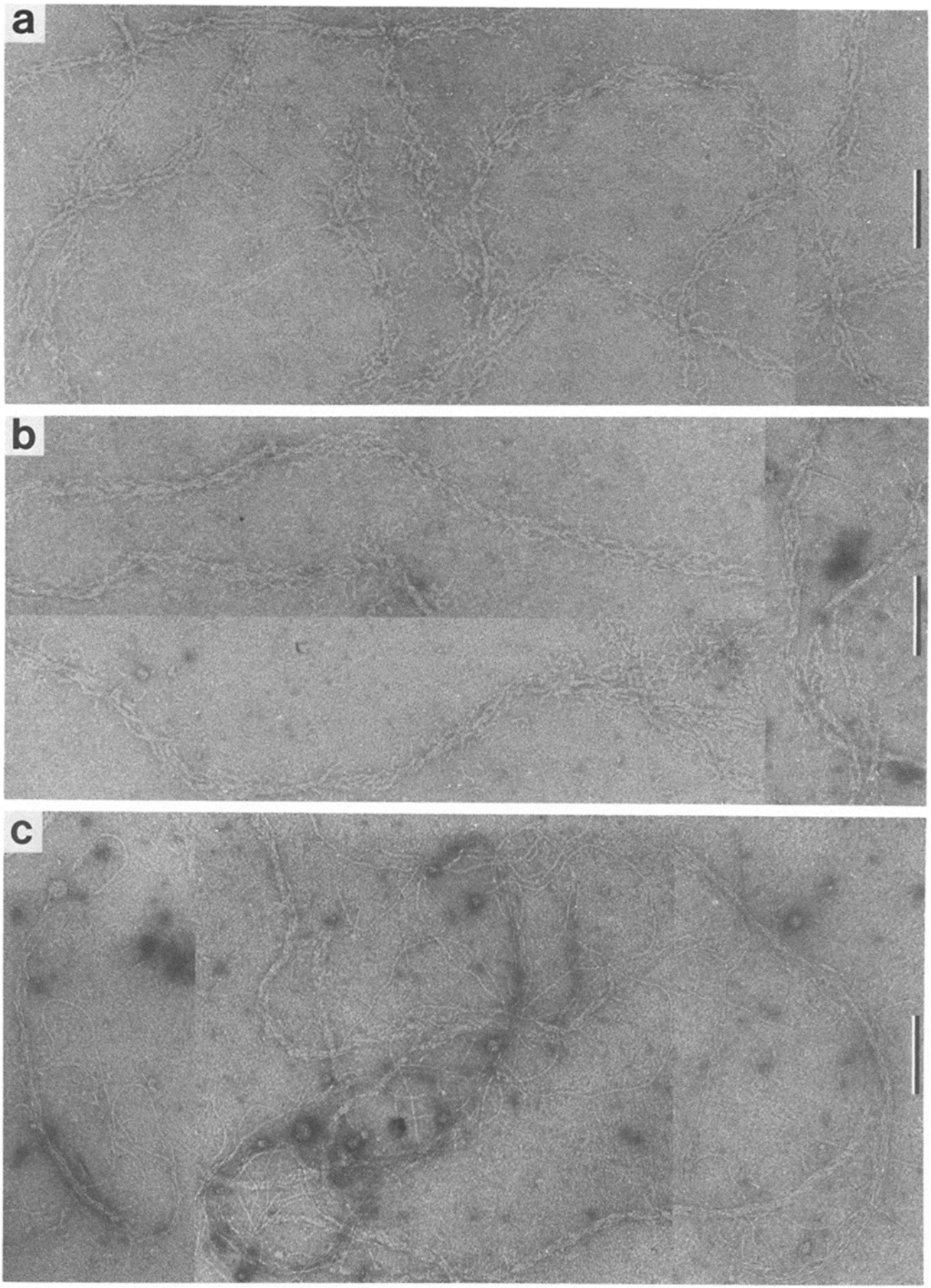
a
b
c

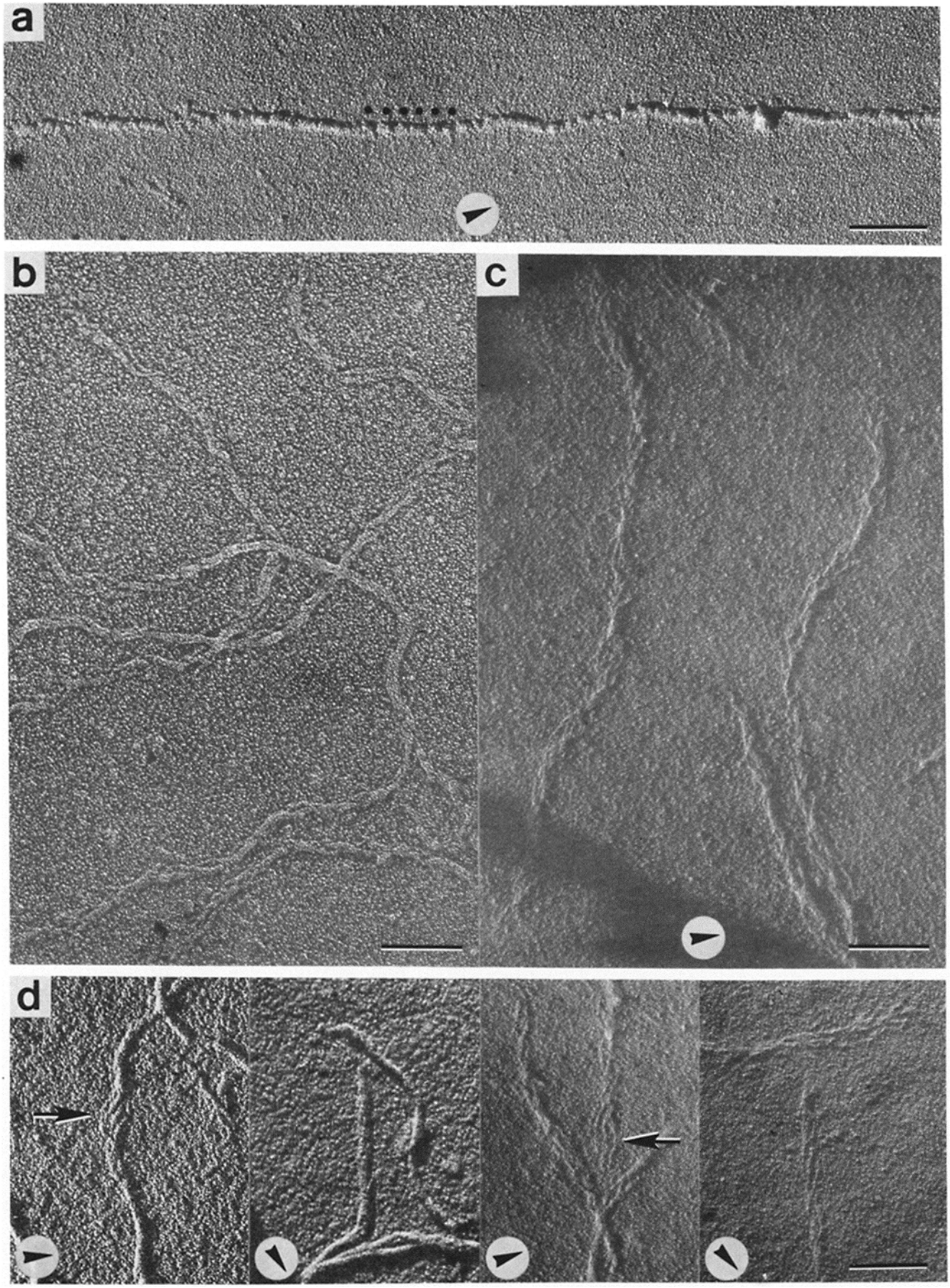
a
b
c
d

several alpha-helical segments (12), are consistent with a four-stranded protofilament unit built as a dimer of interchain double-stranded coiled-coils (12, 51). Finally, the observation that the true protofilament diameter is probably closer to 2.5–3.0 nm (see the section b in Results, and references 9, 16–18) than to 2 nm (e.g. 7, 8) may also be taken as evidence for a four-stranded protofilament, although it is possible that this larger diameter primarily stems from the non-alpha-helical terminal domains of the intermediate filament polypeptides (13), which may contribute more to an increased width of the protofilament unit than to its length (see below).

Steven et al. (19, 20) have studied the distribution of mass in several types of native and in vitro reconstituted intermediate-sized filaments having subunit molecular weights between 50 and 55 kdaltons by scanning transmission electron microscopy (STEM) of unstained specimens. They found that the major class of each intermediate filament type analyzed had an average "linear mass density" of 37 kdaltons/nm. This value results in 32 polypeptides per 10-nm filament cross-section, assuming an average polypeptide molecular weight of 52.5 kdaltons (12, 20) and an average axial repeat of 46 nm (see e.g. reference 19) for the folded polypeptides in the filament. This number is consistent with approximately eleven three-stranded (7, 8) protofilaments as proposed by Steven et al. (19, 20) or with eight four-stranded (12, 51) protofilaments. Our attempts to count the number of protofilaments in unravelling filaments (see Fig. 2*c*) were inconclusive due to extensive tangling and superposition of the protofilaments in such specimens, although in places six to eight protofilaments could be distinguished.

Our results are most compatible with the existence of four 4.5-nm protofibrils per 10-nm filament, as indicated in our schematic model (Fig. 6*a*[III]). This feature of the model is also consistent with the appearance of cross-sections of neurofilaments (52) and skeletin filaments (53), which have revealed "tetragonal" filament profiles. If the number of protofilaments per filament calculated above is correct, the protofibril most likely consists of either three three-stranded or two four-stranded protofilaments. While at present we have no direct evidence regarding this number, preliminary results obtained from unraveling protofibrils are indicative of a two-stranded protofibril (data not shown), which in turn would support a four-stranded protofilament model.

Despite the present lack of detailed information as to the exact packing of the four 4.5-nm protofibrils in the intact 10-nm filament, it is straightforward to build a four-stranded helix having a diameter between 9 and 11 nm. "Compact" association of the four protofibrils gives an outermost diameter of ~9 nm (see Fig. 6*a*[III]), while a more "open" association (not shown) results in an outermost diameter of ~10.5 nm. It is conceivable that such extreme packing arrangements will co-exist and be assumed at periodic intervals along the filament, with intermediate packing arrangements being interspersed. In fact, a regular nodular appearance every 46 nm has been visualized in negatively stained preparations of reconstituted vimentin filaments (19). We observed similar nodes with reconstituted keratin filaments under appropriate preparation conditions (P. Rew and U. Aebi, unpublished data). These nodes may represent positions of compact protofibril association along the filament that may be more resistant to charge-induced swelling or unraveling than the remainder of the filament.

Using images of unstained intermediate filaments that were recorded in a scanning transmission electron microscope, Steven et al. (19, 20) computed a projected width of these filaments of ~15 nm, which is substantially greater than the width we (see Table I) and others (see e.g. references 1–4, 40) have determined by measuring the average stain exclusion profile of intact negatively stained filaments, in our case ~9 nm. While the effective filament width is probably underestimated in the latter cases due to the fact that part of the filament may be buried under the negative stain replica, we think it is highly unlikely that the true value has been underestimated by as much as 5–6 nm. Furthermore, the average width of intact freeze-dried and rotary-shadowed filaments given in Table I, 12.6 nm, is almost certainly an overestimate of the actual filament width, since the measured value has not been corrected for the contribution of the thickness of the metal coat to the measured diameter (25, 34). We have demonstrated here that keratin filaments tend to unravel under a variety of ionic conditions and thereby assume apparent diameters significantly in excess of 10 nm; it is possible that the unstained filaments used by Steven et al. (19, 20) for their width measurements were partially unraveled.

Our measurements of protofibril crossover repeats (Table I) in unraveling filaments (see Figs. 2, *a* and *b*, and 3 *b–d*) are consistent with the protofibrils having a right-handed pitch of ~92 nm. This repeat, as well as a number of other axial repeats that have been reported (19, 32, 33) for different types of intermediate filaments, can be related to the model in Fig. 6*a*. In projection, a four-stranded filament (Fig. 6*a* [III]) should display an axial repeat equal to 1/4 of the 92-nm pitch of the 4.5-nm protofibrils, or 23 nm on average (Fig. 6*b*). This latter repeat has been observed by others (32, 33) and ourselves (see Fig. 3, *a* and Table I) on intact filaments after preparation by glycerol spraying/vacuum drying and metal shadowing. The presence of glycerol may be necessary to give a favorable "decoration" effect (25, 34, 54) that enables visualization of this repeat. Since the protofibrillar substructure of the filaments cannot be resolved by this preparation method (Fig. 3*a* [32, 33]) glycerol-sprayed/vacuum-dried and metal-shadowed filaments should not display a handedness at their 23-nm crossovers unless the four-stranded helix has suffered from anisotropic distortions during specimen prepa-

FIGURE 3 Appearance of keratin filaments after metal-shadowing. (a) Reconstituted callus keratin filaments (1 mg/ml) prepared by glycerol spraying/vacuum drying at room temperature (24, 25) followed by unidirectional shadowing with platinum/carbon. A few 23-nm beaded repeats along the filament have been marked with black dots. (*b*) Reconstituted callus keratin filaments treated with 10 mM Na-phosphate as in Fig. 2*b*, freeze-dried and rotary-shadowed with platinum/carbon. (c) Reconstituted callus keratin filaments prepared in exactly the same way as in *b*, except that they were unidirectionally shadowed with tantalum/tungsten. (*d*) Selected examples of freeze-dried, phosphate-treated keratin filaments unidirectionally shadowed with platinum/carbon (*left*) or tantalum/tungsten (*right*). Note the right-handed twist of the protofibrils in all of these examples. Four protofibrils can sometimes clearly be distinguished (arrows). The arrowheads on white background in a, c, and *d* indicate the direction of metal-shadowing. Bar, 100 nm. × 145,000.

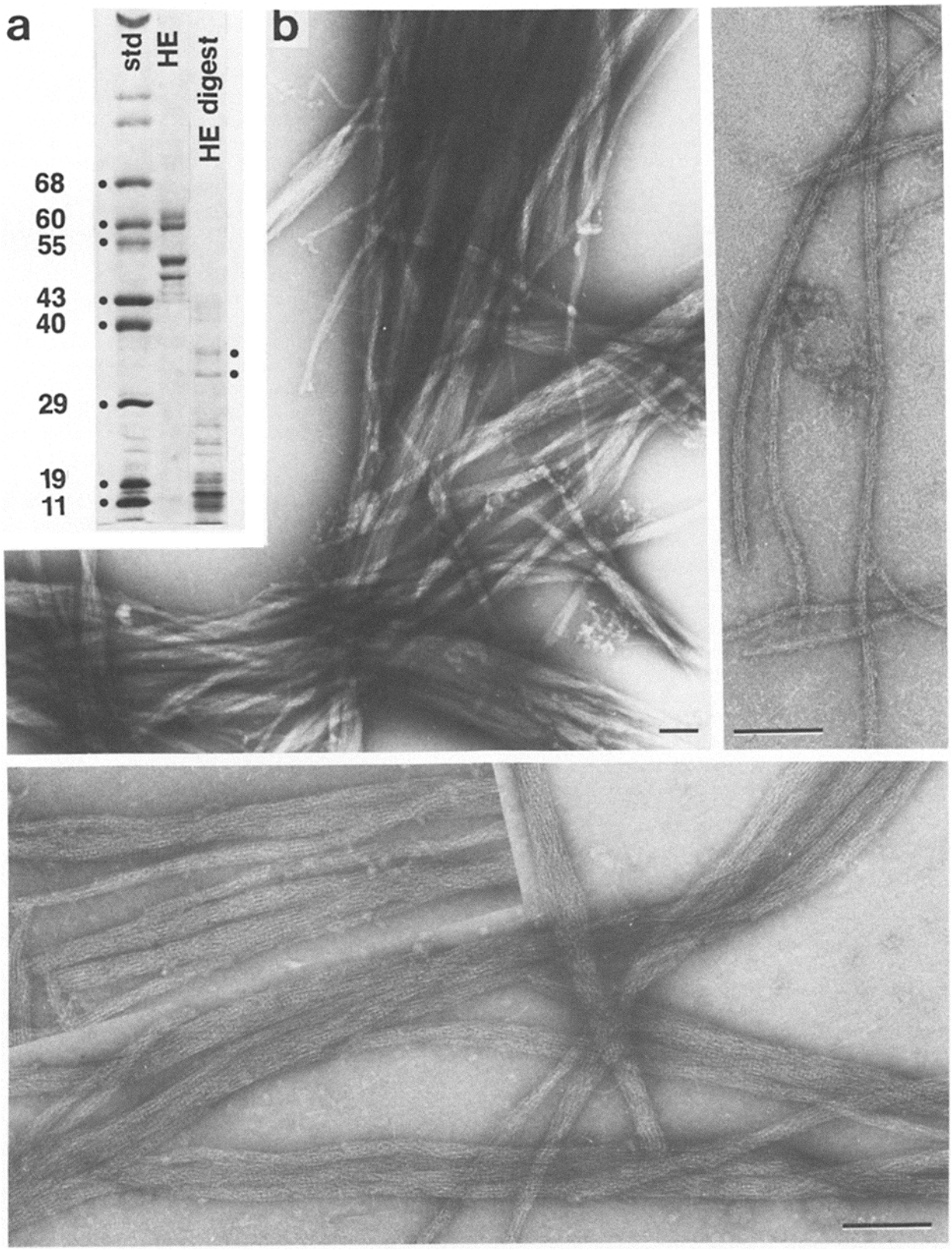

FIGURE 4 Paracrystalline bundles formed from a mixture of keratin extract and trypsin by dialysis against filament reconstitution buffer. (*a*) 10% polyacrylamide SDS gel electrophoresis of standards (see Fig. 1*a*), fresh HE keratin extract and HE keratin extract/trypsin mixture after dialysis. (*b*) Paracrystalline bundles formed from the proteolyzed keratin extract negatively stained with uranyl formate. At high magnification (*right-hand* and *lower* panels), the bundles are seen to consist of laterally aggregated 4.5-nm protofibrils displaying a prominent 5.4-nm axial repeat (see also Fig. 5). Bars, 100 nm. (*b*, *left*) × 70,000; (*b*, *right*) × 155,000. (*c*) × 155,000.

ration. The ambiguous handedness that we have found with such filament preparations (see section c in Results and reference 33) may be due to such collapse phenomena (55). Finally, the 46-nm nodular repeat seen in negatively stained vimentin filaments (19) is equal to half the 92-nm pitch of the protofibrils. The possible relationship of these observed

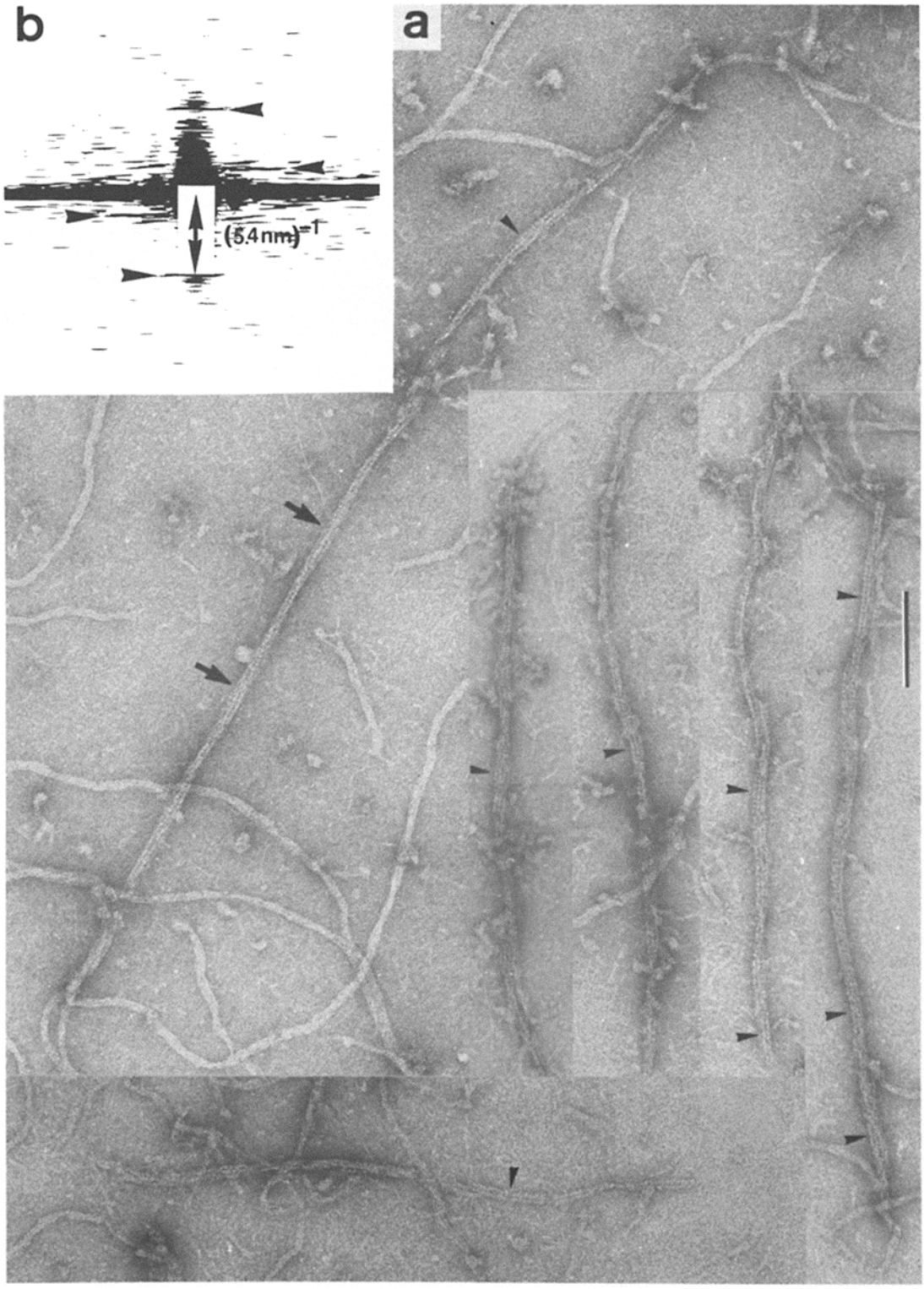

FIGURE 5 Limited proteolysis of keratin filaments that have been immobilized on an EM grid, after which the grid was negatively stained with uranyl formate. (*a*) Electron micrographs containing filament stretches displaying a distinctive protofibrillar substructure (see arrowheads). (*b*) Optical diffraction pattern recorded from the filament stretch marked with two arrows in *a*. The reciprocal spacing of the meridional reflection is indicated with a double-arrow; the near-equatorial arrowheads point to a layer line sampling a 16.2 nm pitch helix of the 4.5-nm protofibrils. Bar, 100 nm. (*a*) × 150,000.

axial repeats in our four-stranded filament model is diagrammed in Fig. 6*b*.

Based on proteolysis patterns, primary sequence data and secondary structure analysis, it has been proposed that all intermediate filament polypeptides—independent of their molecular weight—may be represented by a common topographical model consisting of a 40–45 nm long rodlike middle domain containing several alpha-helical segments that is flanked at both ends by non-alpha-helical terminal domains. It has been suggested that these terminal domains do not

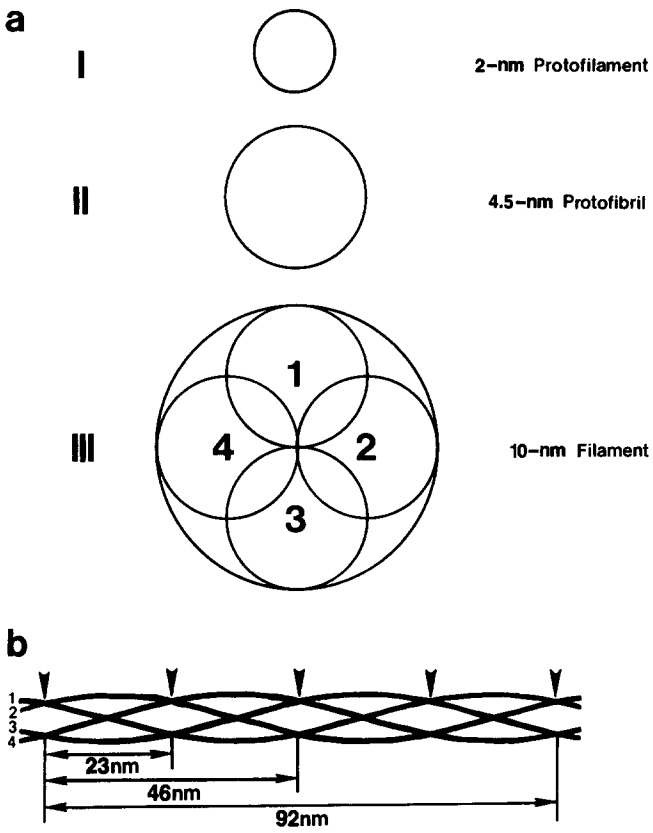

FIGURE 6 Schematic representations of various aspects of the proposed keratin filament model. (a) The three distinct levels of fibrillar organization in the keratin filament displayed as cross-sections: (*I*) the 2-nm protofilament (whose effective diameter is more like 2.5–3.0 nm) consisting of either three or four coiled-coil alpha-helical segments as proposed earlier (5–8, 12, 13, 51); (*II*) the 4.5-nm protofibril made of either three three-standed or two four-stranded protofilaments which are helically twisted around each other; (*III*) the 10-nm filament made of four (*1, 2, 3, 4*) 4.5-nm protofibrils constituting a four-stranded right-handed helix. The association shown here results in an outermost diameter of ~9 nm, however less compact association can give an outermost diameter of ~10.5 nm (not shown). The exact packing arrangement is not known at present. (*b*) Projection of a four-stranded helix made of four 4.5-nm protofibrils each having a 92-nm pitch, demonstrating the occurence of the various axial repeats (i.e., 23 nm, 46 nm, 92 nm) as others (19, 32, 33) and we have observed them.

significantly add to the axial extent of the folded subunit but instead protrude radially from the rodlike middle domain (6–8, 10–13). While the middle domain appears to be rather conserved in size and sequence homology, the size and sequence of the terminal domains varies appreciably among different intermediate filament subunits (10–13).

Reconstitution of keratin extracts in the presence of low levels of trypsin or trypsinization of immobilized keratin filaments on EM grids both yield 4.5-nm protofibrils that exhibit a distinct 5.4-nm axial repeat. This repeat, which has not been visualized in unraveling protofibrils of unproteolyzed filaments and has not been observed previously, may be based on a corresponding repeat in the 2-nm protofilament or ultimately in the primary or secondary structure of the filament polypeptides. Possible mechanisms for generating such an axial repeat include: (*a*) a systematic axial stagger of the polypeptides constituting the protofibril. (*b*) the exact helical organization of the protofibril in terms of the constituent protofilaments (e.g., pitch and number of protofilaments). (*c*) a hitherto undetected regularity in the charge distribution along the surface of the folded subunits. The results of some recent cross-linking experiments impose some constraints on the possible stagger of adjacent polypeptides in the protofilament or protofibril. It was found that adjacent polypeptides in the filament were cross-linked via the same cysteine residue (56), meaning that pairs of adjacent polypeptides have to either be oriented parallel with no stagger or anti-parallel with a fixed stagger that is determined by the axial position of the cross-linked cysteine on the folded polypeptide. The detailed helical organization of the protofibril might be disentangled with the help of Fourier analysis of paracrystalline arrays of proteolyzed protofibrils (see Figs. 4 and 5). Finally, although available primary sequence data from various intermediate filament subunits (10–13, 45–47) have not yet revealed a 5.4-nm repeat, charge periodicities corresponding to a 4.2-nm axial repeat have been noted within the alpha-helical segments of these polypeptides (10, 12, 13, 48–50).

Our finding that low levels of phosphate ions around neutral pH cause in vitro reconstituted keratin filaments to unravel came as a surprise in view of the fact that all vertebrate intermediate filaments are generally thought to be relatively rigid and insoluble structures at physiological ionic strength and pH (2). However, it has been reported previously that 10-nm filaments reconstituted from purified glial fibrillary acidic protein are almost completely solubilized in 1 mM Na-phosphate at pH 8.0 (58). Although we have recently found that neurofilaments unravel in the presence of 1–10 mM Na-phosphate at pH 7.5 (to be published elsewhere), it remains to be determined whether phosphate has a similar unraveling effect on all types of intermediate filaments. The mode of action of phosphate in unraveling some intermediate filaments is speculative. Phosphate may interfere with ionic charges on the surface of the folded filament polypeptides that presumably hold adjacent protofilaments or protofibrils together (13, 50). Alternatively, there may exist a hitherto unknown relationship between the effect of phosphate ions on the structural integrity of intermediate filaments and the fact that all intermediate filament polypeptides so far examined are phosphorylated in vivo and can be phosphorylated in vitro (4). In this regard, it has been found that alteration of the level of phosphorylation of vimentin-type intermediate filaments is temporally related to the alteration in the spatial organization of intermediate filaments during mitosis of cultured mammalian cells (59).

While the tentative keratin filament model proposed here unifies many of the observations and suggestions made previously about the fibrillar substructure of various types of native and in vitro reconstituted 10-nm filaments, it is premature to make firm statements as to its generality. Since all types of intermediate filaments so far analyzed share common chemical and immunological properties (3, 4, 12, 13, 46, 47, 57), it is conceivable that they are also structurally related to one another by a common type of building block such as the 2-nm protofilament and/or the 4.5-nm protofibril. However, it may well turn out that the number and exact association of protofilaments or protofibrils in the filament are species-specific or exhibit a polymorphism even within a particular class of intermediate-sized filaments (19, 20; our own unpublished data).

Finally, we would like to stress that several of the experimental strategies employed here to visualize various aspects of the fibrillar substructure of in vitro reconstituted epidermal cell keratin filaments may also be applicable to the structural dissection of other types of intermediate-sized filaments.

We would like to thank Drs. T. D. Pollard and P. R. Smith for critical reading of this manuscript and making many constructive suggestions.

This work was supported by National Institutes of Health (NIH) Grants GM27765 and GM31940 (to U. Aebi), EY02472 and AM25140 (to T.-T. Sun). U. Aebi and T.-T. Sun were also the recipients of a research award from the Maurice-Muller-Foundation in Switzerland, and an NIH Career Development Award (EY00125), respectively; W. E. Fowler was supported by a Muscular Dystrophy postdoctoral fellowship.

Received for publication 22 March 1983, and in revised form 27 June 1983.

REFERENCES

1. Lazarides, E. 1980. Intermediate filaments as mechanical integrators of cellular space. *Nature (Lond.).* 283:249–256.
2. Anderton, B. H. 1981. Intermediate filaments: a family of homologous structures. *J. Muscle Res. Cell Motil.* 2:141–166.
3. Osborn, M., N. Geisler, G. Shaw, G. Sharp, and K. Weber. 1981. Intermediate filaments. *Cold Spring Harbor Symp. Quant. Biol.* 46:413–429.
4. Lazarides, E. 1982. Intermediate filaments: a chemically heterogeneous, developmentally regulated class of proteins. *Annu. Rev. Biochem.* 51:219–250.
5. Skerrow, D., A. G. Matoltsy, and M. N. Matoltsy. 1973. Isolation and characterization of the alpha helical regions of epidermal prekeratin. *J. Biol. Chem.* 248:4820–4826.
6. Fraser, R. D. B., T. P. MacRae, and E. J. Suzuki, 1976. Structure of the alpha-keratin microfibril. *J. Mol. Biol.* 108:435–452.
7. Steinert, P. M. 1978. Structure of the three-chain unit of the bovine epidermal keratin filament. *J. Mol. Biol.* 123:49–70.
8. Steinert, P. M., W. W. Idler, and R. D. Goldman, 1980. Intermediate filaments of baby hamster kidney (BHK-21) cells and bovine epidermal keratinocytes have similar ultrastructures and subunit domain structures. *Proc. Natl. Acad. Sci. USA* 77:4534–4538.
9. Renner, W., W. W. Franke, E. Schmid, N. Geisler, K. Weber, and E. Mandelkow. 1981. Reconstitution of intermediate-sized filaments from denatured monomeric vimentin. *J. Mol. Biol.* 149:285–306.
10. Geisler, N., E. Kaufmann, and K. Weber. 1982. Proteinchemical characterization of three structurally distinct domains along the protofilament unit of desmin nm filaments. *Cell.* 30:277–286.
11. Hanukoglu, I., and E. Fuchs. 1982. The cDNA sequence of a human epidermal keratin: divergence of sequence but conservation of structure among intermediate filament proteins. *Cell.* 31:243–252.
12. Geisler, N., and K. Weber. 1982. The amino acid sequence of chicken muscle desmin provides a common structural model for intermediate filament proteins. *EMBO (Eur. Mol. Biol. Org.) J.* 1:1649–1656.
13. Steinert, P. M., R. H. Rice, D. R. Roop, B. L. Trus, and A. C. Steven. 1983. Complete amino acid sequence of a mouse epidermal keratin subunit and implications for the structure of intermediate filaments. *Nature (Lond.).* 302:794–800.
14. Skerrow, D. 1974. The structure of prekeratin. *Biochem. Biophys. Res. Commun.* 59:1311–1316.
15. Metuzals, J., and W. E. Mushynski. 1974. Electron microscope and experimental investigations of the neurofilamentous network in Dieters' neurons. Relationship with the cell surface and nuclear pores. *J. Cell Biol.* 61:701–722.
16. Schlaepfer, W. W. 1977. Studies on the isolation and substructure of mammalian neurofilaments. *J. Ultrastruct. Res.* 61:149–157.
17. Krishnan, N., I. R. Kaiserman-Abramof, and R. J. Lasek. 1979. Helical substructure of neurofilaments isolated from myxicola and squid giant axons. *J. Cell Biol.* 82:323–335.
18. Stromer, M. H., T. W. Huiatt, F. L. Richardson, and R. M. Robson. 1981. Disassembly of synthetic 10-nm desmin filaments from smooth muscle into protofilaments. *Eur. J. Cell Biol.* 25:136–143.
19. Steven, A. C., J. Wall, J. Hainfeld, and P. M. Steinert. 1982. Structure of fibroblastic intermediate filaments: analysis by scanning transmission electron microscopy. *Proc. Natl. Acad. Sci. USA* 79:3101–3105.
20. Steven, A. C., J. F. Hainfeld, B. L. Trus, J. S. Wall, and P. M. Steinert, 1983. The distribution of mass in heteropolymer intermediate filaments assembled in vitro: STEM analysis of vimentin/desmin and bovine epidermal keratin. *J. Biol. Chem.* 258:8323–8329.
21. Sun, T.-T., and H. Green. 1978. Keratin filaments of cultured human epidermal cells. *J. Biol. Chem.* 253:2053–2060.
22. Deatherage, J., R. Henderson, and R. J. Capaldi. 1982. Relationship between membrane and cytoplasmic domains in cytochrome c oxidase by electron microscopy in media of different density. *J. Mol. Biol.* 158:501–514.
23. Shotton, D. M., B. E. Burke, and D. Branton. 1979. The molecular structure of human erythrocyte spectrin—biophysical and electron microscopy studies. *J. Mol. Biol.* 131:303–329.
24. Fowler, W. E., and H. P. Erickson, 1979. Trinodular structure of fibrinogen—confirmation by both shadowing and negative stain electron microscopy. *J. Mol. Biol.* 134:241–248.
25. Fowler, W. E., and U. Aebi. 1983. Preparation of single molecules and supramolecular complexes for high resolution metal shadowing. *J. Ultrastruct. Res.* In press.
26. Kistler, J., U. Aebi, and E. Kellenberger. 1977. Freeze-drying and shadowing a two-dimensional periodic specimen. *J. Ultrastruct. Res.* 59:76–86.
27. Smith, P. R. 1980. Freeze-drying specimens for electron microscopy. *J. Ultrastruct. Res.* 72:380–384.
28. Wrigley, N. E. 1968. The lattice spacing of crystalline catalase as an internal standard of length in electron microscopy. *J. Ultrastruct. Res.* 24:454–464.
29. Fukuyama, K., T. Urozuka, R. Caldwell, and W. Epstein. 1978. Divalent cation stimulation of in vitro fiber assembly from epidermal keratin protein. *J. Cell Sci.* 33:255–263.
30. Dale, B. A., K. A. Holbrook, and P. M. Steinert. 1978. Assembly of stratum corneum basic protein and keratin filaments in macrofibrils. *Nature (Lond.).* 276:729–731.
31. Steinert, P. M., J. S. Cantieri, D. C. Teller, J. D. Lonsdale-Eccles, and B. A. Dale. 1981. Characterization of a class of cationic proteins that specifically interact with intermediate filaments. *Proc. Natl. Acad. Sci. USA* 78:4097–4101.
32. Henderson, D., N. Geisler, and K. Weber. 1982. A periodic ultrastructure in intermediate filaments. *J. Mol. Biol.* 155:173–176.
33. Milam, L., and H. P. Erickson. 1982. Visualization of a 21-nm axial periodicity in shadowed keratin filaments and neurofilaments. *J. Cell Biol.* 94:592–596.
34. Heuser, J. 1983. A procedure for freeze-drying molecules adsorbed to mica flakes. *J. Mol. Biol.* In press.
35. Thaler, M., K. Fukuyama, W. L Epstein, and K. A. Fisher. 1980. Comparative studies of keratins isolated from psoriasis and atopic dermatitis. *Invest. Dermatol.* 75:156–158.
36. O'Brien, E., J. Gillis, and J. J. Couch. 1975. Symmetry and molecular arrangement in paracrystals of reconstituted muscle thin filaments. *J. Mol. Biol.* 99:461–475.
37. Fowler, W. E., and U. Aebi. 1982. Polymorphism of actin paracrystals induced by polylysine. *J. Cell Biol.* 93:452–458.
38. Zackroff, R., and R. Goldman. 1979. In vitro assembly of intermediate filaments from baby hamster (BHK-21) cells. *Proc. Natl. Acad. Sci. USA.* 76:6226–6230.
39. Zackroff, R., and R. Goldman. 1980. In vitro reassembly of squid brain intermediate filaments (neurofilaments): purification by assembly/disassembly. *Science (Wash. DC).* 208:1152–1154.
40. Steinert, P. 1981. Intermediate Filaments (IF). *In* Electron Microscopy of Proteins. J. Harris, editor. Academic Press, London. pp. 125–165.
41. Day, A. W., and D. S. Gilbert. 1972. X-ray diffraction pattern of axoplasm. *Biochem. Biophys. Acta.* 285:503–506.
42. Steinert, P. M., W. W. Idler, and S. B. Zimmerman. 1976. Self-assembly of bovine epidermal keratin filaments in vitro. *J. Mol. Biol.* 108:547–567.
43. Steinert, P. M., S. B. Zimmerman, J. M. Starger, and R. D. Goldman. 1978. Ten-nanometer filaments of hamster BHK-21 cells and epidermal keratin filaments have similar structures. *Proc. Natl. Acad. Sci. USA.* 75:6098–6101.
44. Wais-Steider, C., P. A. M. Eagles, D. S. Gilbert, and J. M. Hopkins. 1983. Structural similarities and differences amongst neurofilaments. *J. Mol. Biol.* 165:393–400.
45. Crewther, E. G., L. M. Dowling, K. H. Gough, A. S. Inglis, N. M. McKern, L. G. Sparrow, and E. F. Woods. 1976. *Proc. Int. Wool Text. Res. Conf., 5th Aachen, 1975.* 2:233–242.
46. Geisler, N., and K. Weber. 1981. Comparison of the proteins of two immunologically distinct intermediate-sized filaments by amino acid sequence analysis: desmin and vimentin. *Proc. Natl. Acad. Sci. USA.* 78:4120–4123.
47. Geisler, N., U. Plessmann, and K. Weber. 1982. Related amino acid sequences in neurofilaments and non-neuronal intermediate filaments. *Nature (Lond.).* 296:448–450.
48. Parry, D. A. D., W. G. Crewther, R. D. B. Fraser, and T. P. MacRae. 1977. Structure of alpha-keratin: structural implication of the amino acid sequences of the type I and type II chain segments. *J. Mol. Biol.* 113:449–454.
49. McLachlan, A. D. 1978. Coiled coil formation and sequence regularities in the helical regions of alpha-keratin. *J. Mol. Biol.* 124:297–304.
50. McLachlan, A. D., and M. Stewart. 1982. Periodic charge distribution in the intermediate filament proteins desmin and vimentin. *J. Mol. Biol.* 162:693–698.
51. Ahmadi, B., and P. T. Speakman. 1978. Suberimidate crosslinking shows that a rod-shaped, low cysteine, high helix protein prepared by limited proteolysis of reduced wool has four protein chains. FEBS (*Fed. Eur. Biol. Sci.*) *Lett.* 94:365–367.
52. Wuerker, R. 1970. Neurofilaments and glial filaments. *Tissue & Cell.* 2:1–9.
53. Eriksson, A., and L. Thornell. 1979. Intermediate (skeletin) filaments in heart purkinje fibers. A correlative morphological and biochemical identification with evidence of a cytoskeletal function. *J. Cell Biol.* 80:231–247.
54. Neugebauer, D-Ch., and H. P. Zingsheim. 1978. The two faces of the purple membrane. Structural differences revealed by metal decoration. *J. Mol. Biol.* 123:235–246.
55. Kellenberger, E., and J. Kistler. 1980. The physics of specimen preparation. *In* Unconventional electron microscopy for molecular structure determination. W. Hoppe and R. Mason, editors. pp. 49–79.
56. Quinlan, R. A., and W. W. Franke. 1982. Heteropolymer filaments of vimentin and desmin in vascular smooth muscle tissue and cultured baby hamster kidney cells demonstrated by chemical crosslinking. *Proc. Natl. Acad. Sci. USA.* 79:3452–3456.
57. Pruss, R. M., R. Mirsky, M. C. Raff, R. Thorpe, A. J. Dowdling, and B. H. Anderton. 1981. All classes of intermediate filaments share a common antigenic determinant defined by a monoclonal antibody. *Cell.* 27:419–428.
58. Rueger, D. C., J. S. Huston, D. Dahl, and A. Bignami. 1979. Formation of 100Å filaments from purified glial fibrillary acidic protein in vitro. *J. Mol. Biol.* 135:53–68.
59. Evans, R. M., and L. M. Fink. 1982. An alteration in the phosphorylation of vimentin-type intermediate filaments is associated with mitosis in cultured mammalian cells. *Cell.* 29:43–52.